Elastic scattering and breakup reactions of the mirror nuclei ^{12}B and ^{12}N on ^{208}Pb using *ab initio* structure inputs

K. Wang,[1,2] Y. Y. Yang,[1,2,*] Jin Lei,[3,†] A. M. Moro,[4,5] V. Guimarães,[6] J. G. Li,[1,2] F. F. Duan,[1] Z. Y. Sun,[1,2] G. Yang,[1,2] D. Y. Pang,[7] S. W. Xu,[1] J. B. Ma,[1] P. Ma,[1] Z. Bai,[1] Q. Liu,[8] J. L. Lou,[9] H. J. Ong,[1,2] B. F. Lv,[1] S. Guo,[1,2] M. Kumar Raju,[1,10] X. H. Wang,[1] R. H. Li,[1] X. X. Xu,[1,2] Z. Z. Ren,[3] Y. H. Zhang,[1,2] X. H. Zhou,[1,2] Z. G. Hu,[1,2] and H. S. Xu[1,2]
(RIBLL Collaboration)

[1]*CAS Key Laboratory of High Precision Nuclear Spectroscopy, Institute of Modern Physics, Chinese Academy of Sciences, Lanzhou 730000, China*
[2]*School of Nuclear Science and Technology, University of Chinese Academy of Sciences, Beijing 100080, China*
[3]*School of Physics Science and Engineering, Tongji University, Shanghai 200092, China*
[4]*Departamento de FAMN, Universidad de Sevilla, Apartado 1065, 41080 Sevilla, Spain*
[5]*Instituto Interuniversitario Carlos I de Física Teórica y Computacional (iC1), Apartado 1065, 41080 Sevilla, Spain*
[6]*Instituto de Física, Universidade de São Paulo, Rua do Matão, 1371, São Paulo 05508-090, São Paulo, Brazil*
[7]*School of Physics and Beijing Key Laboratory of Advanced Nuclear Materials and Physics, Beihang University, Beijing 100191, China*
[8]*School of physics and Optoelectronic Engineering, Anhui University, Hefei 230601, China*
[9]*School of Physics and State Key Laboratory of Nuclear Physics and Technology, Peking University, Beijing 100871, China*
[10]*Department of Physics, GITAM School of Science, GITAM University, Visakhapatnam 530045, India*

(Received 25 July 2023; accepted 11 January 2024; published 29 January 2024)

The angular distributions for the elastic scattering and breakup reactions of the mirror nuclei ^{12}B and ^{12}N on a ^{208}Pb target, at incident energies of 255 MeV and 343 MeV, respectively, were measured at HIRFL-RIBLL. The elastic scattering and breakup angular distributions of the halolike nucleus ^{12}N ($S_p = 0.601$ MeV) have been measured simultaneously. Elastic scattering cross sections were accurately reproduced by continuum discretized coupled channel calculations, which did not exhibit any significant Coulomb rainbow suppression. We have analyzed the energy and angular distributions of inclusive ^{11}B and ^{11}C fragments, produced by direct reaction processes, taking into account the contributions from both elastic breakup (EBU) and nonelastic breakup (NEB). Since the breakup data is inclusive with respect to the final state of the core nucleus, the contribution of each of these core states was calculated separately and then the corresponding cross sections added together using as weights the spectroscopic factors for each configuration computed with the *ab initio* no-core shell model. The results were found to be mostly consistent with the experimental data and, furthermore, demonstrate that EBU is highly dependent on the binding energy, while the results of NEB show no clear effect.

DOI: 10.1103/PhysRevC.109.014624

I. INTRODUCTION

The investigation of light, weakly bound nuclei has garnered considerable attention due to their exotic structures and reaction dynamics, with a strong interplay between the structural characteristics and dynamic processes of these nuclei [1–7]. Elastic scattering and breakup reactions are pivotal for probing the anomalous surface structures found in neutron-rich nuclei such as ^{6,8}He, ^{11}Li, and ^{11}Be. Notably, elastic scattering angular distributions of neutron-rich nuclei on heavy targets show pronounced suppression of the Coulomb-nuclear interference peak and enhanced absorption at backward angles, leading to substantial total reaction cross sections [8]. The interaction of these nuclei with targets has been described by incorporating couplings to both bound and continuum states, not only near the Coulomb barrier but also at energies several times above it [9–16]. The breakup of weakly bound nuclear systems, facilitated by the decoupling of low-binding valence particles, plays a crucial role in both the structural and dynamic aspects of nuclear reactions.

While there is a substantial body of work on neutron-rich systems, the dynamics involving proton-rich projectiles remain less understood, making the breakup mechanisms of such systems particularly intriguing. Previous experiments have largely focused on ^{8}B and ^{17}F projectiles to explore reaction dynamics [17–35]. Recent studies with the brunnian ^{10}C projectile suggest that, although structural influences are significant, the coupling effects are less pronounced compared to those induced by neutron-rich nuclei [36–38]. For the ^{8}B nucleus, the influence of breakup reactions and halo structure is significant, while for ^{10}C, the cluster structure plays a more dominant role in the elastic scattering angular distributions. To deepen our understanding of the reaction dynamics driven by

*Corresponding author: yangyanyun@impcas.ac.cn
†Corresponding author: jinl@tongji.edu.cn

proton-rich projectiles, additional data across various targets and a broad energy spectrum are essential.

The ^{12}N nucleus, characterized by a valence proton in a p-wave orbital with a low binding energy to the ^{11}C core ($S_p = 0.601$ MeV), emerges as a promising candidate for a proton-halo system [39,40]. The effective root-mean-square radius of ^{12}N, determined to be 2.47(7) fm from interaction cross section measurements at the Lawrence Berkeley Laboratory [41], is comparable to those of other $A = 12$ isobars, suggesting nuanced differences in the structural properties and reaction dynamics of these isotopes.

In the realm of nuclear reaction studies, the total reaction cross section serves as a fundamental observable for probing nuclear sizes and structures. For the proton-rich nucleus ^{12}N, measurements on a Si target at approximately 40 A MeV have revealed a notably large total reaction cross section, significantly surpassing that of the stable isotope ^{12}C, drawing parallels with observations made for ^{8}B as documented in Ref. [42]. This enhancement in the reaction cross section for ^{12}N is indicative of its extended nuclear matter distribution, akin to that seen in known halo nuclei.

Further investigations into the reaction cross sections of ^{12}N and its mirror nucleus ^{12}B were carried out at the Heavy Ion Research Facility in Lanzhou (HIRFL) using the Radioactive Ion Beam Line in Lanzhou (RIBLL), at beam energies of 34.9 and 36.2 MeV/u, respectively [43–45]. The application of the Glauber model to these measurements yielded a matter radius (R_m) of 2.52 fm for ^{12}N, suggesting the presence of a proton halo with a radius (R_h) of 4.18 fm. Conversely, the mirror nucleus ^{12}B exhibited a more compact structure with a shorter root-mean-square radius of 2.33 fm. These contrasting radii not only reflect the differences in the internal structure between the mirror nuclei but also underscore the unique characteristic of ^{12}N as a candidate for proton-halo systems.

The neutron-rich ^{12}B and the proton-rich ^{12}N nuclei, mirror partners with identical spin-parity $J^\pi = 1^+$ in their ground states, exhibit markedly different one-nucleon separation energies ($S_n = 3.370$ MeV for ^{12}B and $S_p = 0.601$ MeV for ^{12}N). While elastic scattering data for ^{12}N has yet to be reported, there has been only a single measurement for ^{12}B [46]. This study introduces the inaugural measurement of angular distributions for elastic scattering of both ^{12}B and ^{12}N on a ^{208}Pb target at energies approximately five times their respective Coulomb barriers.

Additionally, we have measured the angular distributions of inclusive ^{11}B and ^{11}C fragments, which are products of direct reactions involving ^{12}B and ^{12}N, respectively. The analysis of our data employed the optical model with double-folding potentials for elastic scattering, continuum discretized coupled channels (CDCC) calculations to assess the elastic breakup, and the Ichimura, Austern, and Vincent (IAV) model to account for nonelastic breakup contributions [47]. A crucial component of our analysis was the application of spectroscopic factors from *ab initio* no-core shell model calculations [48], which helped to clarify the role of core excited states in the inclusive breakup cross sections.

The paper is organized as follows. A description of the experimental setup and data analyses procedure is given in Sec. II. The experimental results and calculations together with the corresponding discussions are presented in Sec. III. In Sec. IV, a brief summary is given.

II. EXPERIMENT AND DATA ANALYSES

The elastic scattering and breakup measurements with the ^{12}B and ^{12}N radioactive beams were conducted at the National Laboratory of Heavy Ion Research of the Institute of Modern Physics of the Chinese Academy of Sciences (IMPCAS). These secondary radioactive ion beams were produced by fragmentation of a primary 59.5 MeV/nucleon $^{16}O^{8+}$ beam on a ^{9}Be target (4.5 mm thick for ^{12}B and 2.0 mm thick for ^{12}N) and purified by magnetic rigidity with RIBLL at HIRFL. The average intensities for ^{12}B and ^{12}N beams were approximately 2×10^4 and 9×10^2 pps, with purities of 93% and 8%, respectively. The beam energies at the center of the ^{208}Pb target (12.24 mg/cm^2 thick self-supporting) were about $E_{\rm lab} = 255$ and 343 MeV for ^{12}B and ^{12}N, respectively. Two 50-μm-thick plastic scintillator detectors, located at the second and fourth focal points of RIBLL, were used to obtain the time-of-flight (TOF) information. The magnetic rigidity, together with time of flight, enabled a complete particle identification. Two double-sided silicon strip detectors (DSSDs), 48×48 mm^2 (16 × 16 pixels), 669 mm and 69 mm upstream from the ^{208}Pb target, were used to provide the precise position and direction of the incident beam particles on event by event basis. Four silicon telescopes (∼150 μm DSSDs as ΔE and ∼1500 μm square silicon detectors as E detectors), mounted 267 mm from the lead target, covering an angular range from 3° to 27°, allowed the measurement of the elastically scattered particles and reaction products. A detailed description of the experimental setup and data analysis is given in Refs. [49–51].

Typical two-dimensional particle identification spectra are shown in Fig. 1(a), for a time window on ^{12}B, and Fig. 1(b) on ^{12}N. Owing to the excellent resolution of TOF signals, which is better than 2 ns (full width at half maximum), it can be seen that both ^{12}B and ^{12}N particles are well separated and no elastically scattered beams of ^{11}B or ^{11}C are mixed with the products coming from reactions. The experimental elastic scattering angular distributions for ^{12}B + ^{208}Pb at $E_{\rm lab} = 255$ MeV and ^{12}N + ^{208}Pb at $E_{\rm lab} = 343$ MeV are shown in Fig. 2 normalized to the Rutherford scattering cross sections. Typical Fresnel diffraction patterns can be seen for both systems. For the breakup processes, however, in Fig. 1 there is a band of events starting from the elastic scattering locus with the same ΔE energy while the E energy decreases. These events are elastic scattering events for which the E energy is not correctly measured due to the channeling effect in the E detector [52]. The ^{11}C products coming from reactions are clearly identified, while for ^{11}B these background events must be removed. Here we take the similar procedure as used in Ref. [53]. The same gate used for selecting ^{11}B, dashed red line in Fig. 1(a), was shifted so as to include a similar fraction of background events as in the ^{11}B gate, shown by black solid line. The background-subtracted experimental cross sections for the breakup processes were then obtained event by event. The resulting angular distributions of the produced ^{11}B and ^{11}C fragments, presumably stemming from breakup and transfer processes, are shown in Fig. 3 (inclusive breakup). To

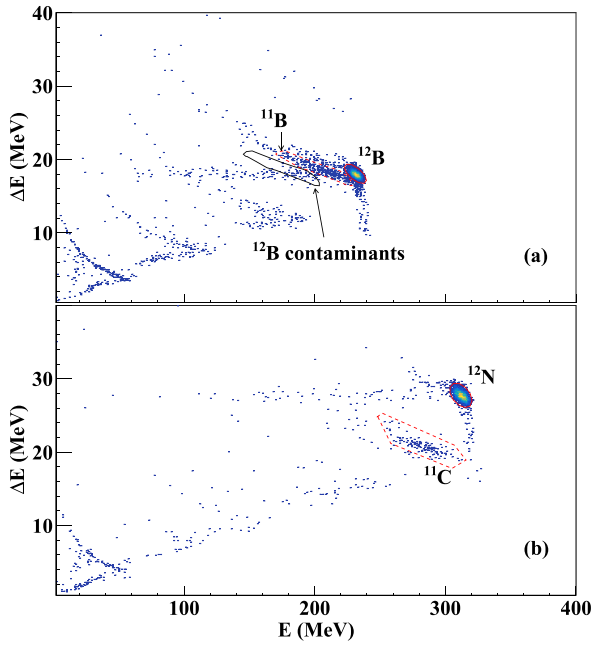

FIG. 1. (a) Calibrated two-dimensional $\Delta E - E$ particle identification spectrum for ^{12}B obtained by one of the silicon telescopes, which covers an angular range from 3° to 20°; (b) the same spectrum but with a time window on ^{12}N.

be noted, to obtain the background-subtracted energy distribution of ^{11}B, the energy of these background events must be shifted by the same E as the one used to produce the black gate before subtraction.

III. RESULTS AND DISCUSSIONS

First, the obtained angular distributions for the elastic scattering of ^{12}B and ^{12}N on a ^{208}Pb target were analyzed

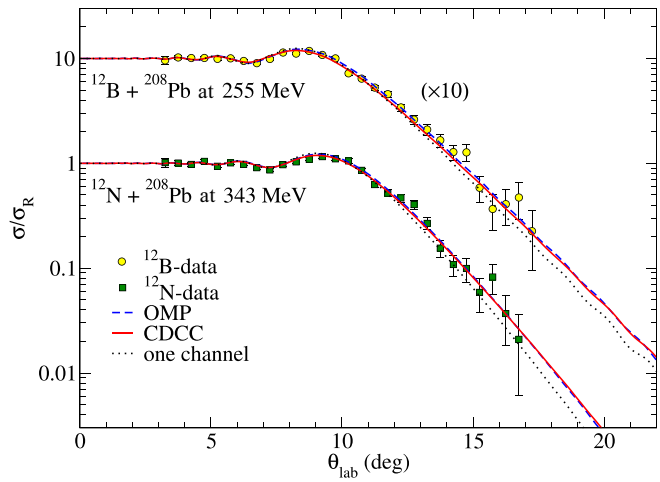

FIG. 2. Elastic scattering angular distributions for ^{12}B + ^{208}Pb at $E_{lab} = 255$ MeV and ^{12}N + ^{208}Pb at $E_{lab} = 343$ MeV, as well as their comparisons with calculations. Error bars are due only to statistical uncertainty.

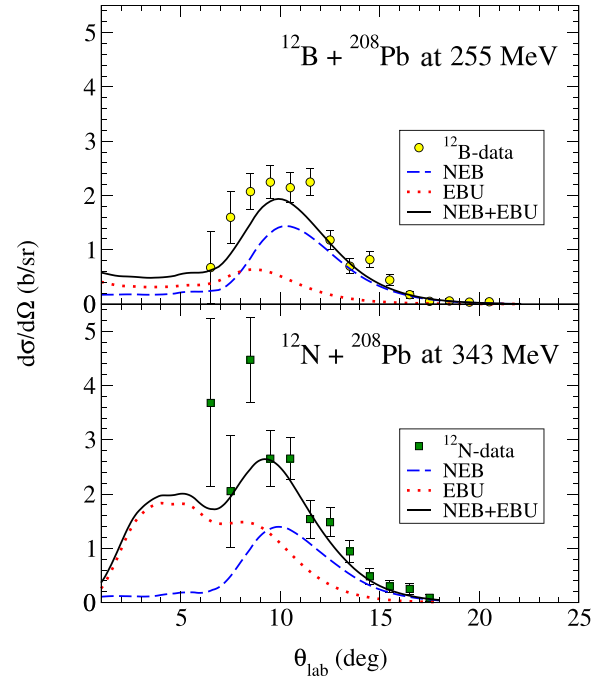

FIG. 3. Experimental angular distributions (AD) for ^{11}B products in ^{12}B + ^{208}Pb at $E_{lab} = 255$ MeV and ^{11}C products in ^{12}N + ^{208}Pb at $E_{lab} = 343$ MeV, and also the comparisons with calculations. The data have been rebinned due to the low statistics compared with the elastic scattering events. Error bars are statistical only.

with the traditional optical model (OMP). We employed the systematic nucleus-nucleus potential by Xu and Pang [54], which employs Bruyeres Jeuk'enne-Lejeune-Mahaux's nucleon-nucleus model potentials [55,56]. The required proton and neutron densities were obtained from Hartree-Fock calculations based on the SkX interaction [57]. The results of these calculations are shown in Fig. 2 by dashed lines. Overall, they give a good description of the data within the reported error bars. The derived total reaction cross sections are 3582 and 3623 mb for ^{12}B + ^{208}Pb and ^{12}N + ^{208}Pb, respectively.

Additionally, CDCC calculations assuming a simple three-body model consisting of an inert core and a valence nucleon for the $^{12}\text{B} \rightarrow {}^{11}\text{B} + n$ and $^{12}\text{N} \rightarrow {}^{11}\text{C} + p$ projectiles were performed. The bound and continuum states of the ^{12}B and ^{12}N systems were generated using a Woods-Saxon potential with diffuseness $a = 0.7$ fm and the radius adjusted to reproduce the rms predicted by a Hartree-Fock calculation with the Skyrme SkX interaction. This yields $R_0 = 2.86$ fm and $R_0 = 3.04$ fm for the ^{12}B and ^{12}N systems, respectively, assuming in both cases a $p_{1/2}$ configuration for the valence nucleon. The potential depth was adjusted for each projectile to ensure the correct separation energy ($S_n = 3.370$ MeV and $S_p = 0.601$ MeV for ^{12}B and ^{12}N, respectively). For each projectile, the continuum spectrum was discretized into energy bins for each angular momentum configuration between the valence and core particles, up to a maximum excitation energy of $E_{max} = 35$ MeV. The maximum orbital angular momentum was $\ell_{max} = 4$ and a sufficiently large model space

was selected to guarantee the convergence of the elastic scattering cross section. The nucleon-target interaction was taken from the systematic potential of Koning and Delaroche [58], whereas for the core-target potential we used the global single-folding nucleus-nucleus potential of Xu and Pang [54].

These CDCC calculations, shown in Fig. 2 by solid lines, give a fairly good description of the experimental elastic scattering angular distributions, showing only modest effects of the coupling to the continuum for both systems, as can be inferred from the comparison of these full CDCC calculations with one-channel calculations in which couplings to breakup channels are omitted (dotted lines). These results are in line with those for ^{8}B [22,23,25–27].

The Ichimura-Austern-Vincent (IAV) model, established in 1985 [47], provides a comprehensive framework for the simultaneous investigation of breakup and transfer reactions [60–62], offering a deeper understanding of nuclear reaction mechanisms. It distinguishes between elastic breakup (EBU), where both the projectile and target emerge unexcited, and nonelastic breakup (NEB), which encompasses scenarios where the projectile's core remains intact while the valence nucleon engages further with the target. Incorporating this approach, we have analyzed the angular distributions from the inclusive processes ^{208}Pb(^{12}B,^{11}BX) and ^{208}Pb(^{12}N,^{11}CX), presented in Fig. 3. In general, the data will encompass contributions from EBU as well as NEB. To quantify the NEB contributions with precision, we have applied the DWBA form of the IAV model (DWBA-IAV), which allows for a detailed dissection of these intricate processes and furthers our comprehension of the underlying dynamics in such proton-rich nuclear systems.

One should note that the ^{12}B and ^{12}N ground states contain significant admixtures of core excited components. Therefore, the dissociation of ^{12}B into $^{11}\mathrm{B}+n$ and ^{12}N into $^{11}\mathrm{C}+p$ channels may end up in a final state in which the remaining residual cores (^{11}B and ^{11}C, respectively) are left in an excited state. Since the different core states could not be resolved experimentally, for a meaningful comparison with the data, we performed several calculations, each of which corresponds to a given ground state configuration of the projectile, characterized by a single-particle configuration of the valence particle bound to a given state of the core with an effective separation energy. In addition to the core ground state, we considered the core excited states at $E_x(1/2^-) = 2.125$ MeV, $E_x(5/2^-) = 4.445$ MeV, and $E_x(3/2^-) = 5.02$ MeV for ^{11}B and $E_x(1/2^-) = 2$ MeV, $E_x(5/2^-) = 4.319$ MeV, and $E_x(3/2^-) = 4.804$ MeV for ^{11}C. The calculated breakup cross sections are then multiplied by the corresponding spectroscopic factors, which account for the weight of each configuration in the projectile ground state, and added incoherently. Note that this procedure ignores possible transitions between different core states during the reaction but, insofar as the total breakup cross section is concerned, this approximation is expected to be justified.

The spectroscopic factors for the considered excited states were calculated with the *ab initio* no-core shell model (NCSM) method [48]. These calculations are performed without the core assumption, in contrast to the traditional shell model (SM), in which truncated model spaces, with inner frozen core, are assumed. The model space was as large as possible to guarantee the convergence of the results within the computational limitations [48,63,64]. An outstanding feature of the NCSM calculations is its competent handling of the internucleon correlations. The NCSM calculation was based on the Daejeon16 interaction [65], which provides accurate descriptions of light nuclei. The list of the considered configurations for ^{11}B and ^{11}C and their associated spectroscopic factors computed by the NCSM calculations are shown in Tables I and II, respectively, and compared with the results using variational Monte Carlo (VMC) [59] and traditional shell model (SM). The calculated cross sections for EBU and NEB contributions for each state within the measured angles in Fig. 3 are also listed. The measured cross sections were obtained by integrating the cross sections of each angle in Fig. 3 assuming a uniform distribution within each bin.

The dotted, dashed, and solid lines in Fig. 4 represent the EBU (CDCC), NEB (DWBA-IAV) contributions and their incoherent sum, respectively. Although the calculations slightly underestimate the data, some conclusions can be drawn. For the neutron-rich ^{12}B projectile the inclusive cross section is dominated by the NEB component, while for ^{12}N the EBU

TABLE I. Summary of inclusive breakup results obtained for $^{12}\mathrm{B}+^{208}\mathrm{Pb}$, showing the EBU cross section from CDCC calculations, NEB cross section using the DWBA-IAV model, and the measured cross sections, all within the measured angles $6^\circ \leqslant \theta_{\mathrm{lab}} < 21^\circ$. Spectroscopic factors of the considered ^{11}B configurations evaluated through shell model calculations (with the WBT interaction) and the *ab initio* VMC [59] and NCSM formalisms are also shown.

^{11}B state	lsj	NEB+EBU (mb)	VMC SF	σ_{VMC} (mb)	SM SF	σ_{SM} (mb)	NCSM SF	σ_{NCSM} (mb)	σ_{exp} (mb)
3/2-	$p_{3/2}$	155 + 79	0.152	159	0.117	193	0.073	157	291(17)
3/2-	$p_{1/2}$		0.527		0.708		0.599		
1/2-	$p_{3/2}$	108 + 31	0.270	42	0.293	41	0.269	39	
1/2-	$p_{1/2}$		0.034		0.005		0.010		
5/2-	$p_{3/2}$	73 + 14	0.021	2	0.308	27	0.235	20	
3/2-	$p_{3/2}$	73 + 12	0.336	30	0.391	34	0.307	31	
3/2-	$p_{1/2}$		0.023		0.017		0.054		
Sum				233		295		247	

TABLE II. Summary of inclusive breakup results obtained for ^{12}N+^{208}Pb showing the EBU cross section from CDCC calculations, NEB cross section using the DWBA-IAV model, and the measured cross sections, all within the measured angles $6^\circ \leqslant \theta_{\rm lab} < 18^\circ$. Spectroscopic factors of the considered ^{11}C configurations evaluated through shell model utilizing the WBT interaction, as well as from the *ab initio* NCSM formalism, are also listed.

^{11}C state	lsj	NEB+EBU (mb)	SM SF	$\sigma_{\rm SM}$ (mb)	NCSM SF	$\sigma_{\rm NCSM}$ (mb)	$\sigma_{\rm exp}$ (mb)
3/2-	$p_{3/2}$	122 + 256	0.118	312	0.071	250	374(33)
3/2-	$p_{1/2}$		0.708		0.591		
1/2-	$p_{3/2}$	92 + 42	0.293	40	0.274	38	
1/2-	$p_{1/2}$		0.005		0.009		
5/2-	$p_{3/2}$	75 + 14	0.293	26	0.243	22	
3/2-	$p_{3/2}$	72 + 11	0.392	34	0.310	30	
3/2-	$p_{1/2}$		0.017		0.056		
Sum			412		340		

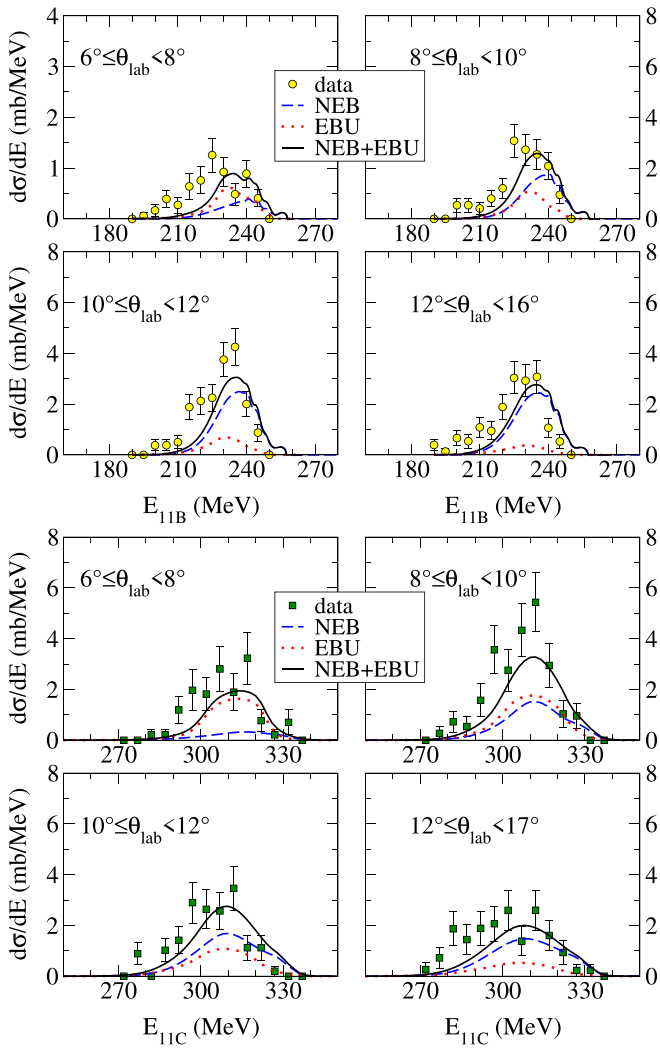

FIG. 4. Experimental breakup differential cross section, as a function of the ^{11}B and ^{11}C laboratory energies, for selected values of the scattering angle and comparisons with calculations. Error bars are statistical only.

is the dominant contribution. This can be understood by the fact that ^{12}N is less bound giving a higher EBU contribution, whereas the NEB contribution is less sensitive to the separation energy [66].

To provide further insight into the reaction dynamics, we also investigated the energy distributions of the ^{11}B and ^{11}C fragments in Fig. 4. The energy spectra were corrected for the energy losses in the target and dead layers of the detectors. The calculations include, as before, the EBU and NEB contributions. The calculations reproduce very well the energy of the peak position in the ^{11}C case and they slightly overestimate it in the case of ^{11}B. The important feature is that the combined contributions adequately explain the measured distributions, with a small underestimation of the magnitude, as also noted in the corresponding angular distributions.

IV. SUMMARY

In this work, we have presented angular distributions for the elastic scattering and inclusive breakup of the mirror nuclei ^{12}B and ^{12}N, which are respectively neutron rich and proton rich. The elastic scattering data were analyzed using the optical model, employing the Xu and Pang systematic nucleus-nucleus potential built with Hartree-Fock densities employing the SkX interaction. The elastic distributions were also found to be well described by continuum discretized coupled channels (CDCC) calculations based on a two-body model of the projectile (^{12}B = ^{11}B + 1n and ^{12}N = ^{11}C + 1p). These calculations revealed also a modest effect of the coupling to the breakup channels on the elastic cross sections.

Inclusive breakup angular and energy distributions, corresponding to the processes ^{208}Pb(^{12}B,^{11}BX) and ^{208}Pb(^{12}N,^{11}CX), were also extracted and analyzed. These distributions were assumed to contain both elastic and nonelastic breakup contributions, which were respectively evaluated with the CDCC and IAV methods. Because the experiment did not allow the separation of the different core states produced after the 1n or 1p dissociation, the contribution of each final core state was calculated separately

and summed incoherently using as weights the spectroscopic factors derived from *ab initio* no-core shell model (NCSM) calculations. The final results showed an overall good agreement with the experimental distributions, except for some slight underestimation of the absolute magnitude. Interestingly, the NEB contribution was found to be of similar magnitude in both reactions, whereas the EBU part is enhanced in the ^{12}N reaction, which turns out to dominate the inclusive breakup cross section below the grazing angle. This result is attributed to the greater sensitivity of the EBU to the separation energy of the projectile (due to its peripheral character) combined with the smaller separation energy of the ^{12}N nucleus.

This comparative study of mirror systems has shed light on the influence of proton and neutron asymmetry in nuclei on their elastic and breakup reactions, enhancing our understanding of the interplay between nuclear structure and reaction dynamics.

ACKNOWLEDGMENTS

We would like to acknowledge the staff of HIRFL for the operation of the cyclotron and those of RIBLL for their friendly collaboration. This work was financially supported by the National Natural Science Foundation of China (Grants No. 12122511, No. 12105330, No. 12105204, No. 12035011, and No. 11975167), the National Key R&D Program of China (Grant No. 2018YFA0404403), the Fundamental Research Funds for the Central Universities, and the Youth Innovation Promotion Association CAS (Grant No. 2020411). A.M.M. is supported by the Spanish Ministerio de Ciencia, Innovación y Universidades (including FEDER funds) under Project No. FIS2017-88410-P and by the European Union's Horizon 2020 research and innovation program under Grant Agreement No. 654002. V.G. would like to thank Sao Paulo Research Foundation (FAPESP) (Grant No. 16/17612-7) and CNPq (Grant No. 303769/2021-1).

[1] L. F. Canto, P. R. S. Gomes, R. Donangelo, J. Lubian, and M. S. Hussein, Phys. Rep. **596**, 1 (2015).
[2] J. Kolata, V. Guimarães, and E. Aguilera, Eur. Phys. J. A **52**, 123 (2016).
[3] K. Hagino, K. Ogata, and A. Moro, Prog. Part. Nucl. Phys. **125**, 103951 (2022).
[4] Z. Ren, B. Chen, Z. Ma, and G. Xu, Phys. Rev. C **53**, R572 (1996).
[5] Z. Ren, A. Faessler, and A. Bobyk, Phys. Rev. C **57**, 2752 (1998).
[6] S. Kaur, R. Kanungo, W. Horiuchi, G. Hagen, J. D. Holt, B. S. Hu, T. Miyagi, T. Suzuki, F. Ameil, J. Atkinson, Y. Ayyad, S. Bagchi, D. Cortina-Gil, I. Dillmann, A. Estradé, A. Evdokimov, F. Farinon, H. Geissel, G. Guastalla, R. Janik *et al.*, Phys. Rev. Lett. **129**, 142502 (2022).
[7] S. J. Novario, D. Lonardoni, S. Gandolfi, and G. Hagen, Phys. Rev. Lett. **130**, 032501 (2023).
[8] L. F. Canto, V. G. aes, J. Lubian, and M. S. Hussein, Eur. Phys. J. A **56**, 281 (2020).
[9] A. Chatterjee, A. Navin, A. Shrivastava, S. Bhattacharyya, M. Rejmund, N. Keeley, V. Nanal, J. Nyberg, R. G. Pillay, K. Ramachandran, I. Stefan, D. Bazin, D. Beaumel, Y. Blumenfeld, G. de France, D. Gupta, M. Labiche, A. Lemasson, R. Lemmon, R. Raabe *et al.*, Phys. Rev. Lett. **101**, 032701 (2008).
[10] G. Marquínez-Durán, N. Keeley, K. W. Kemper, R. S. Mackintosh, I. Martel, K. Rusek, and A. M. Sánchez-Benítez, Phys. Rev. C **95**, 024602 (2017).
[11] A. Di Pietro, G. Randisi, V. Scuderi, L. Acosta, F. Amorini, M. J. G. Borge, P. Figuera, M. Fisichella, L. M. Fraile, J. Gomez-Camacho, H. Jeppesen, M. Lattuada, I. Martel, M. Milin, A. Musumarra, M. Papa, M. G. Pellegriti, F. Perez-Bernal, R. Raabe, F. Rizzo *et al.*, Phys. Rev. Lett. **105**, 022701 (2010).
[12] M. Cubero, J. P. Fernández-García, M. Rodríguez-Gallardo, L. Acosta, M. Alcorta, M. A. G. Alvarez, M. J. G. Borge, L. Buchmann, C. A. Diget, H. A. Falou, B. R. Fulton, H. O. U. Fynbo, D. Galaviz, J. Gómez-Camacho, R. Kanungo, J. A. Lay, M. Madurga, I. Martel, A. M. Moro, I. Mukha *et al.*, Phys. Rev. Lett. **109**, 262701 (2012).
[13] J. P. Fernández-García, M. Cubero, M. Rodríguez-Gallardo, L. Acosta, M. Alcorta, M. A. G. Alvarez, M. J. G. Borge, L. Buchmann, C. A. Diget, H. A. Falou, B. R. Fulton, H. O. U. Fynbo, D. Galaviz, J. Gómez-Camacho, R. Kanungo, J. A. Lay, M. Madurga, I. Martel, A. M. Moro, I. Mukha *et al.*, Phys. Rev. Lett. **110**, 142701 (2013).
[14] V. Pesudo, M. J. G. Borge, A. M. Moro, J. A. Lay, E. Nácher, J. Gómez-Camacho, O. Tengblad, L. Acosta, M. Alcorta, M. A. G. Alvarez, C. Andreoiu, P. C. Bender, R. Braid, M. Cubero, A. Di Pietro, J. P. Fernández-García, P. Figuera, M. Fisichella, B. R. Fulton, A. B. Garnsworthy *et al.*, Phys. Rev. Lett. **118**, 152502 (2017).
[15] F. Duan, Y. Yang, K. Wang, A. Moro, V. Guimarães, D. Pang, J. Wang, Z. Sun, J. Lei, A. Di Pietro, X. Liu, G. Yang, J. Ma, P. Ma, S. Xu, Z. Bai, X. Sun, Q. Hu, J. Lou, X. Xu *et al.*, Phys. Lett. B **811**, 135942 (2020).
[16] F. F. Duan, Y. Y. Yang, J. Lei, K. Wang, Z. Y. Sun, D. Y. Pang, J. S. Wang, X. Liu, S. W. Xu, J. B. Ma, P. Ma, Z. Bai, Q. Hu, Z. H. Gao, X. X. Xu, C. J. Lin, H. M. Jia, N. R. Ma, L. J. Sun, D. X. Wang *et al.* (RIBLL Collaboration), Phys. Rev. C **105**, 034602 (2022).
[17] A. Barioni, J. C. Zamora, V. Guimarães, B. Paes, J. Lubian, E. F. Aguilera, J. J. Kolata, A. L. Roberts, F. D. Becchetti, A. Villano, M. Ojaruega, and H. Jiang, Phys. Rev. C **84**, 014603 (2011).
[18] V. Morcelle, R. Lichtenthäler, A. Lépine-Szily, V. Guimarães, K. C. C. Pires, J. Lubian, D. R. Mendes Junior, P. N. de Faria, J. J. Kolata, F. D. Becchetti, H. Jiang, E. F. Aguilera, D. Lizcano, E. Martinez-Quiroz, and H. Garcia, Phys. Rev. C **95**, 014615 (2017).
[19] E. F. Aguilera, E. Martinez-Quiroz, D. Lizcano, A. Gómez-Camacho, J. J. Kolata, L. O. Lamm, V. Guimarães, R. Lichtenthäler, O. Camargo, F. D. Becchetti, H. Jiang, P. A. DeYoung, P. J. Mears, and T. L. Belyaeva, Phys. Rev. C **79**, 021601(R) (2009).
[20] J. Lubian, T. Correa, E. F. Aguilera, L. F. Canto, A. Gomez-Camacho, E. M. Quiroz, and P. R. S. Gomes, Phys. Rev. C **79**, 064605 (2009).

[21] M. Mazzocco, N. Keeley, A. Boiano, C. Boiano, M. La Commara, C. Manea, C. Parascandolo, D. Pierroutsakou, C. Signorini, E. Strano, D. Torresi, H. Yamaguchi, D. Kahl, L. Acosta, P. Di Meo, J. P. Fernandez-Garcia, T. Glodariu, J. Grebosz, A. Guglielmetti, Y. Hirayama *et al.*, Phys. Rev. C **100**, 024602 (2019).

[22] Y. Y. Yang, J. S. Wang, Q. Wang, D. Pang, J. B. Ma, M. R. Huang, J. L. Han, P. Ma, S. L. Jin, Z. Bai, Q. Hu, L. Jin, J. B. Chen, N. Keeley, K. Rusek, R. Wada, S. Mukherjee, Z. Y. Sun, R. F. Chen, X. Y. Zhang *et al.*, Phys. Rev. C **87**, 044613 (2013).

[23] Y. Y. Yang, X. Liu, D. Y. Pang, D. Patel, R. F. Chen, J. S. Wang, P. Ma, J. B. Ma, S. L. Jin, Z. Bai, V. Guimarães, Q. Wang, W. H. Ma, F. F. Duan, Z. H. Gao, Y. C. Yu, Z. Y. Sun, Z. G. Hu, S. W. Xu, S. T. Wang *et al.*, Phys. Rev. C **98**, 044608 (2018).

[24] A. Pakou, L. Acosta, P. D. O'Malley, S. Aguilar, E. F. Aguilera, M. Baines, D. Bardayan, F. D. Becchetti, C. Boomershine, M. Brodeur, F. Cappuzzello, S. Carmichael, L. Caves, E. Chávez, C. Flores-Vázquez, A. Gula, J. J. Kolata, B. Liu, D. J. Marín-Lámbarri, F. F. Morales *et al.*, Phys. Rev. C **102**, 031601(R) (2020).

[25] R. Spartà, A. Di Pietro, P. Figuera, O. Tengblad, A. Moro, I. Martel, J. Fernández-García, J. Lei, L. Acosta, M. Borge, G. Bruni, J. Cederkäll, T. Davinson, J. Ovejas, L. Fraile, D. Galaviz, J. Halkjaer Jensen, B. Jonson, M. La Cognata, A. Perea *et al.*, Phys. Lett. B **820**, 136477 (2021).

[26] K. Wang, Y. Y. Yang, A. M. Moro, V. Guimarães, J. Lei, D. Y. Pang, F. F. Duan, J. L. Lou, J. C. Zamora, J. S. Wang, Z. Y. Sun, H. J. Ong, X. Liu, S. W. Xu, J. B. Ma, P. Ma, Z. Bai, Q. Hu, X. X. Xu, Z. H. Gao, and H. S. Xu (RIBLL Collaboration), Phys. Rev. C **103**, 024606 (2021).

[27] L. Yang, C. J. Lin, H. Yamaguchi, A. M. Moro, N. R. Ma, D. X. Wang, K. J. Cook, M. Mazzocco, P. W. Wen, S. Hayakawa, J. S. Wang, Y. Y. Yang, G. L. Zhang, Z. Huang, A. Inoue, H. M. Jia, D. Kahl, A. Kim, M. S. Kwag, M. L. Commara *et al.*, Nat. Commun. **13**, 7193 (2022).

[28] J. Liang, J. Beene, H. Esbensen, A. Galindo-Uribarri, J. Gomez del Campo, C. Gross, M. Halbert, P. Mueller, D. Shapira, D. Stracener, and R. Varner, Phys. Lett. B **491**, 23 (2000).

[29] J. F. Liang, J. R. Beene, H. Esbensen, A. Galindo-Uribarri, J. Gomez del Campo, C. J. Gross, M. L. Halbert, P. E. Mueller, D. Shapira, D. W. Stracener, I. J. Thompson, and R. L. Varner, Phys. Rev. C **65**, 051603(R) (2002).

[30] J. F. Liang, J. R. Beene, A. Galindo-Uribarri, J. Gomez del Campo, C. J. Gross, P. A. Hausladen, P. E. Mueller, D. Shapira, D. W. Stracener, R. L. Varner, J. D. Bierman, H. Esbensen, and Y. Larochelle, Phys. Rev. C **67**, 044603 (2003).

[31] M. Romoli, E. Vardaci, M. Di Pietro, A. De Francesco, A. De Rosa, G. Inglima, M. La Commara, B. Martin, D. Pierroutsakou, M. Sandoli, M. Mazzocco, T. Glodariu, P. Scopel, C. Signorini, R. Bonetti, A. Guglielmetti, F. Soramel, L. Stroe, J. Greene, A. Heinz *et al.*, Phys. Rev. C **69**, 064614 (2004).

[32] C. Signorini, D. Pierroutsakou, B. Martin, M. Mazzocco, T. Glodariu, R. Bonetti, A. Guglielmetti, M. L. Commara, M. Romoli, M. Sandoli, E. Vardaci, H. Esbensen, F. Farinon, P. Molini, C. Parascandolo, F. Soramel, S. Sidortchuk, and L. Stroe, Eur. Phys. J. A **44**, 63 (2010).

[33] M. Mazzocco, C. Signorini, D. Pierroutsakou, T. Glodariu, A. Boiano, C. Boiano, F. Farinon, P. Figuera, D. Filipescu, L. Fortunato, A. Guglielmetti, G. Inglima, M. La Commara, M. Lattuada, P. Lotti, C. Mazzocchi, P. Molini, A. Musumarra, A. Pakou, C. Parascandolo *et al.*, Phys. Rev. C **82**, 054604 (2010).

[34] G. L. Zhang, G. X. Zhang, C. J. Lin, J. Lubian, J. Rangel, B. Paes, J. L. Ferreira, H. Q. Zhang, W. W. Qu, H. M. Jia, L. Yang, N. R. Ma, L. J. Sun, D. X. Wang, L. Zheng, X. X. Liu, X. T. Chu, J. C. Yang, J. S. Wang, S. W. Xu *et al.*, Phys. Rev. C **97**, 044618 (2018).

[35] L. Yang, C. Lin, H. Yamaguchi, J. Lei, P. Wen, M. Mazzocco, N. Ma, L. Sun, D. Wang, G. Zhang, K. Abe, S. Cha, K. Chae, A. Diaz-Torres, J. Ferreira, S. Hayakawa, H. Jia, D. Kahl, A. Kim, M. Kwag *et al.*, Phys. Lett. B **813**, 136045 (2021).

[36] Y. Y. Yang, J. S. Wang, Q. Wang, D. Y. Pang, J. B. Ma, M. R. Huang, P. Ma, S. L. Jin, J. L. Han, Z. Bai, L. Jin, J. B. Chen, Q. Hu, R. Wada, S. Mukherjee, Z. Y. Sun, R. F. Chen, X. Y. Zhang, Z. G. Hu, X. H. Yuan *et al.*, Phys. Rev. C **90**, 014606 (2014).

[37] V. Guimarães, E. N. Cardozo, V. B. Scarduelli, J. Lubian, J. J. Kolata, P. D. O'Malley, D. W. Bardayan, E. F. Aguilera, E. Martinez-Quiroz, D. Lizcano, A. Garcia-Flores, M. Febbraro, C. C. Lawrence, J. Riggins, R. O. Torres-Isea, P. N. de Faria, D. S. Monteiro, E. S. Rossi, and N. N. Deshmukh, Phys. Rev. C **100**, 034603 (2019).

[38] R. Linares, M. Sinha, E. N. Cardozo, V. Guimarães, G. V. Rogachev, J. Hooker, E. Koshchiy, T. Ahn, C. Hunt, H. Jayatissa, S. Upadhyayula, B. Roeder, A. Saastomoinen, J. Lubian, M. Rodríguez-Gallardo, J. Casal, K. C. C. Pires, M. Assunçao, Y. Penionzhkevich, and S. Lukyanov, Phys. Rev. C **103**, 044613 (2021).

[39] T. Inomata, H. Akimune, I. Daito, H. Ejiri, H. Fujimura, Y. Fujita, M. Fujiwara, M. N. Harakeh, K. Ishibashi, H. Kohri, N. Matsuoka, S. Nakayama, A. Tamii, M. Tanaka, H. Toyokawa, M. Yoshimura, and M. Yosoi, Phys. Rev. C **57**, 3153 (1998).

[40] T. Minamisono, T. Ohtsubo, K. Sato, S. Takeda, S. Fukuda, T. Izumikawa, M. Tanigaki, T. Miyake, T. Yamaguchi, N. Nakamura, H. Tanji, K. Matsuta, M. Fukuda, and Y. Nojiri, Phys. Lett. B **420**, 31 (1998).

[41] A. Ozawa, I. Tanihata, T. Kobayashi, D. Hirata, O. Yamakawa, K. Omata, N. Takahashi, T. Shimoda, K. Sugimoto, D. Olson, W. Christie, and H. Wieman, Nucl. Phys. A **583**, 807 (1995).

[42] R. Warner, H. Thirumurthy, J. Woodroffe, F. Becchetti, J. Brown, B. Davids, A. Galonsky, J. Kolata, J. Kruse, M. Lee, A. Nadasen, T. O'Donnell, D. Roberts, R. Ronningen, C. Samanta, P. Schwandt, J. von Schwarzenberg, M. Steiner, K. Subotic, J. Wang *et al.*, Nucl. Phys. A **635**, 292 (1998).

[43] W. L. Zhan, J. W. Xia, H. W. Zhao, G. Q. Xiao, Y. J. Yuan, H. S. Xu, K. D. Man, P. Yuan, D. Q. Gao, X. T. Yang, M. T. Song, X. H. Cai, X. D. Yang, Z. Y. Sun, W. X. Huang, Z. G. Gan, and B. W. Wei, Nucl. Phys. A **805**, 533c (2008).

[44] J. X. Li, P. P. Liu, J. S. Wang, Z. G. Hu, R. S. Mao, C. Li, R. F. Chen, Z. Y. Sun, H. S. Xu, G. Q. Xiao, and Z. Y. Guo, Chin. Phys. Lett. **27**, 032501 (2010).

[45] J. X. Li, P. P. Liu, J. S. Wang, Z. G. Hu, R. S. Mao, Z. Y. Sun, C. Li, R. F. Chen, H. S. Xu, G. Q. Xiao, and Z. Y. Guo, Chin. Phys. C **34**, 452 (2010).

[46] E. O. N. Zevallos, V. Guimarães, E. N. Cardozo, J. Lubian, R. Linares, R. L. Filho, K. C. C. Pires, O. C. B. Santos, S. Appannababu, E. Crema, J. Alcantara-Núñez, A. L. Lara, Y. S. Villamizar, U. Umbelino, N. Added, M. Assuncao, V. Morcelle, and D. S. Monteiro, Phys. Rev. C **99**, 064613 (2019).

[47] M. Ichimura, N. Austern, and C. M. Vincent, Phys. Rev. C **32**, 431 (1985).

[48] B. R. Barrett, P. Navrátil, and J. P. Vary, Prog. Part. Nucl. Phys. **69**, 131 (2013).
[49] K. Wang, Y. Y. Yang, V. Guimarães, D. Y. Pang, F. F. Duan, Z. Y. Sun, J. Lei, G. Yang, S. W. Xu, J. B. Ma, Q. Liu, Z. Bai, H. J. Ong, B. F. Lv, S. Guo, X. H. Wang, R. H. Li, M. K. Raju, Z. G. Hu, and H. S. Xu (RIBLL Collaboration), Phys. Rev. C **105**, 054616 (2022).
[50] Y. Yang, J. Wang, Q. Wang, J. Ma, M. Huang, J. Han, P. Ma, S. Jin, Z. Bai, Q. Hu, L. Jin, J. Chen, R. Wada, Z. Sun, R. Chen, X. Zhang, Z. Hu, X. Yuan, X. Cao, Z. Xu *et al.*, Nucl. Instrum. Methods Phys. Res., A **701**, 1 (2013).
[51] F. F. Duan, Y. Y. Yang, B. T. Hu, J. S. Wang, Z. H. Gao, X. Q. Liu, D. Patel, P. Ma, J. B. Ma, S. Y. Jin, Z. Bai, Q. Hu, G. Yang, X. X. Sun, N. R. Ma, L. J. Sun, H. M. Jia, X. X. Xu, and C. J. Lin, Nucl. Sci. Technol. **29**, 165 (2018).
[52] B. R. Appleton, C. Erginsoy, and W. M. Gibson, Phys. Rev. **161**, 330 (1967).
[53] A. Di Pietro, A. Moro, J. Lei, and R. de Diego, Phys. Lett. B **798**, 134954 (2019).
[54] Y. P. Xu and D. Y. Pang, Phys. Rev. C **87**, 044605 (2013).
[55] E. Bauge, J. P. Delaroche, and M. Girod, Phys. Rev. C **58**, 1118 (1998).
[56] E. Bauge, J. P. Delaroche, and M. Girod, Phys. Rev. C **63**, 024607 (2001).
[57] B. A. Brown, Phys. Rev. C **58**, 220 (1998).
[58] A. Koning and J. Delaroche, Nucl. Phys. A **713**, 231 (2003).
[59] https://www.phy.anl.gov/theory/research/overlaps/ (accessed on September 20, 2021).
[60] T. Udagawa, Y. J. Lee, and T. Tamura, Phys. Rev. C **39**, 47 (1989).
[61] G. Potel, G. Perdikakis, B. V. Carlson, M. C. Atkinson, W. H. Dickhoff, J. E. Escher, M. S. Hussein, J. Lei, W. Li, A. O. Macchiavelli, A. M. Moro, F. M. Nunes, S. D. Pain, and J. Rotureau, Eur. Phys. J. A **53**, 178 (2017).
[62] J. Lei and A. M. Moro, Phys. Rev. C **95**, 044605 (2017).
[63] J. G. Li, N. Michel, B. S. Hu, W. Zuo, and F. R. Xu, Phys. Rev. C **100**, 054313 (2019).
[64] J. Li, C. A. Bertulani, and F. Xu, Phys. Rev. C **105**, 024613 (2022).
[65] A. Shirokov, I. Shin, Y. Kim, M. Sosonkina, P. Maris, and J. Vary, Phys. Lett. B **761**, 87 (2016).
[66] A. M. Moro and J. Lei, Few-Body Syst. **57**, 319 (2016).